This article was downloaded by:
On: *25 January 2011*
Access details: *Access Details: Free Access*
Publisher *Taylor & Francis*
Informa Ltd Registered in England and Wales Registered Number: 1072954 Registered office: Mortimer House, 37-41 Mortimer Street, London W1T 3JH, UK

Liquid Crystals
Publication details, including instructions for authors and subscription information:
http://www.informaworld.com/smpp/title~content=t713926090

Synthesis, characterisation and mesomorphic properties of unsymmetrical N-(o-hydroxybenzylidene)-N'-(4-n-alkoxybenzylidene)azines and their copper (II) complexes

Bachcha Singh[a]; Ashwini Pandey[a]
[a] Department of Chemistry, Faculty of Science, Banaras Hindu University, Varanasi, India

Online publication date: 12 January 2010

To cite this Article Singh, Bachcha and Pandey, Ashwini(2010) 'Synthesis, characterisation and mesomorphic properties of unsymmetrical N-(o-hydroxybenzylidene)-N'-(4-n-alkoxybenzylidene)azines and their copper (II) complexes', Liquid Crystals, 37: 1, 57 — 67
To link to this Article: DOI: 10.1080/02678290903362857
URL: http://dx.doi.org/10.1080/02678290903362857

PLEASE SCROLL DOWN FOR ARTICLE

Full terms and conditions of use: http://www.informaworld.com/terms-and-conditions-of-access.pdf

This article may be used for research, teaching and private study purposes. Any substantial or systematic reproduction, re-distribution, re-selling, loan or sub-licensing, systematic supply or distribution in any form to anyone is expressly forbidden.

The publisher does not give any warranty express or implied or make any representation that the contents will be complete or accurate or up to date. The accuracy of any instructions, formulae and drug doses should be independently verified with primary sources. The publisher shall not be liable for any loss, actions, claims, proceedings, demand or costs or damages whatsoever or howsoever caused arising directly or indirectly in connection with or arising out of the use of this material.

Liquid Crystals,
Vol. 37, No. 1, January 2010, 57–67

Taylor & Francis
Taylor & Francis Group

Synthesis, characterisation and mesomorphic properties of unsymmetrical N-(*o*-hydroxybenzylidene)-N′-(4-n-alkoxybenzylidene)azines and their copper (II) complexes

Bachcha Singh* and Ashwini Pandey

Department of Chemistry, Faculty of Science, Banaras Hindu University, Varanasi – 221005, India

(Received 2 July 2009; final form 24 September 2009)

A new series of mesogenic unsymmetrical azines, N-(*o*-hydroxybenzylidene)-N′-(4-n-alkoxybenzylidene)azines, $HOC_6H_4CH{=}N{-}N{=}CHC_6H_4OC_mH_{2m+1}$ (m = 6, 7, 8, 9, 10, 11, 12, 14 and 16) and their copper (II) complexes have been prepared. They were characterised by elemental analyses, Fourier transform infrared (FT-IR), far infrared (IR), ^{1}H and ^{13}C nuclear magnetic resonance (NMR) spectra, ultraviolet (UV)-visible, electron spin resonance (ESR) and magnetic susceptibility measurements. The copper (II) complexes are square planar and the unpaired electron is present in the dx^2–y^2 orbital. The mesomorphic properties of these compounds were investigated by differential scanning calorimetry and polarising optical microscopy. All of the unsymmetrical azines, except m = 7, exhibit mesogenic nature. The azine (m = 8) shows monotropic nematic mesophase, whereas all other azines exhibit features of a smectic A mesophase in the cooling cycle. The copper (II) complexes of the azines show only an isotropic phase at higher temperatures (~180°C) and no mesogenic nature is observed.

Keywords: differential scanning calorimetry; monotropic nematic mesophase; smectic A mesophase; polarising optical microscopy

Downloaded At: 14:08 25 January 2011

1. Introduction

Azines are a class of compounds that undergo a wide variety of chemical processes that have interesting chemical properties. Azines and pyridyl-substituted azines have been used extensively as ligands for the design and synthesis of novel organometallic compounds [1, 2]. Azines are a 2,3-diaza analogue of butadiene (>C=N–N=C<). The two imino bonds that make up the azine moiety can be considered polar acceptor groups oriented in opposite directions, since they are joined by an N–N bond. These characteristics of azines, when bonded to two aryl rings that contain donor and acceptor groups, respectively, make them ideal candidates for non-linear optics (NLO) materials. Among their useful properties, azines are receiving interest for their potential in bond formation reactions [3, 4], biological properties [5–8], the design of liquid crystals [9–16] and other materials applications [17–19]. The acetophenone azines have been investigated in detail by Chen *et al.* [20, 21] and Glaser *et al.* [22], both experimentally and theoretically.

Centore and Garzillo [12] reported the structural and theoretical analysis of some mesogenic bis(phenylene) azines containing a methyl group on the azine system and strong donor–acceptor groups on the phenylene ring.

Symmetric azines having mesomorphism were reported by Deun *et al.* [23] in which the rare earth (e.g. lanthanum chloride) promotes decomposition of the hydrazide ligands. A series of azine-based liquid crystals with high clearing points were synthesised by Wilfrid and Glenn [24].

Chudgar *et al.* [25] reported a series of azine-type liquid crystals with an ester group and lateral substituents in the rigid core and alkoxy end groups. Wei *et al.* [26] reported two series of new symmetric azine-type liquid crystals, 4,4′-(4-alkylbenzoyloxy)benzalazine and 4,4′-(4-alkoxybenzoyloxy)benzalazine, that contain only ester groups in their linear mesogenic core and alkyl or alkoxy end groups. The end groups of liquid crystals had an effect on their mesomorphic properties. The series with alkoxy end groups exhibited both smectic A (SmA) and nematic mesophases, whereas the series with alkyl end groups showed only a nematic mesophase at their lower analogues and showed both SmA and nematic properties at their higher analogues.

Recently, the mesomorphic properties of 4,4′-dialkoxy-2,2′-dihydroxy benzalazines were reported [27]. It was found that the mesomorphic properties of the 4,4′-dialkoxy-2,2′-dihydroxybenzalazines are highly dependent on the length of the alkoxy chains, i.e. K–N–I for n = 1–3, K–N–SmC–I for n = 4–8 and K–SmC–I for n = 9–18, where SmC represents smectic C. The crystal structure of 4,4′-dioctyloxy-2,2′-dihydroxybenzalazine has also been reported [28]. Centore *et al.* [17] reported asymmetric azines that show both nematic and smectic phases.

It is evident from a literature survey that few reports are available on the synthesis, characterisation

*Corresponding author. Email: bsinghbhu@rediffmail.com

ISSN 0267-8292 print/ISSN 1366-5855 online
© 2010 Taylor & Francis
DOI: 10.1080/02678290903362857
http://www.informaworld.com

and mesomorphic properties of unsymmetrical azines. We report here the synthesis, characterisation and the mesomorphic properties of a new series of liquid crystalline unsymmetrical N-(*o*-hydroxybenzylidene)-N′-(4-n-alkoxybenzylidene)azines, $HOC_6H_4CH{=}N{-}N{=}CHC_6H_4OC_mH_{2m+1}$ (m = 6, 7, 8, 9, 10, 11, 12, 14, 16) and their copper (II) complexes.

2. Experimental details

2.1 Materials

Salicylaldehyde, hydrazine monohydrate, 4-hydroxybenzaldehyde and bromoalkanes, purchased from Aldrich Chemicals, USA, were used as received. All other solvents and reagents were purchased commercially and used after purification.

2.2 Techniques

Elemental analyses were performed on a CE-440 Exeter Analytical CHN analyser. IR spectra (4000–100 cm^{-1}) were recorded on a Varian 3100 Fourier transform infrared (FT-IR) Excalibur series spectrophotometer. ^1H and ^{13}C nuclear magnetic resonance (NMR) spectra were obtained on a JEOL FT-NMR AL 300 MHz spectrometer using tetramethylsilane as the internal standard. Electronic spectra were recorded on an ultraviolet (UV)-1700 Pharma Spec. Shimadzu UV–visible spectrophotometer. Room temperature magnetic susceptibility measurements were performed on a Cahn Faraday balance using $Co[Hg(SCN)_4]$ as standard. The magnetic susceptibility was corrected for diamagnetism using Pascal's constants. The electron spin resonance (ESR) spectrum has been recorded on a Varian, USA E-112 X band ESR spectrometer at room temperature by using tetra-cyanoethylene (TCNE) as the g marker (g = 2.00277). Differential scanning calorimetry (DSC) thermograms were recorded with a Mettler Toledo TC 15 TA differential scanning calorimeter at the rate of 10.0 K min^{-1} under a nitrogen atmosphere using spec pure grade indium as standard by taking samples in close-lid aluminium pans. The transition temperatures from DSC have been determined with an accuracy of ±0.1 K. The mesophase type was identified by visual comparison with known phase standards using an HT 30.01 NTT 268 Lomo polarising optical microscope (POM) fitted with a hot stage with temperature controlling accuracy of 0.1 K. The copper content in the complexes was determined using an atomic absorption spectrophotometer (ASH Corp.).

2.3 Synthesis of compounds

2.3.1 Synthesis of salicylhydrazone (2)

Salicylhydrazone was prepared by adding salicylaldehyde **(1)** (1.07 ml, 10 mmol) to an ice-cold ethanol (15 ml) solution of hydrazine hydrate (0.49 ml, 10 mmol) in drops with continuous stirring. A fast exothermic reaction occurred with the formation of a white precipitate, which was filtered immediately and washed with ethanol. The compound was recrystallised from the hot chloroform solution. Yield: 74%, m.p. 97–98°C (Lit. m.p. 97–98°C). IR (KBr, cm^{-1}): 3481 (OH), 3383 ν_a (N–H), 3287 ν_s (N–H), 1617 (C=N), 1576 (Ph), 1028 (N–N). ^1H NMR ($CDCl_3$, TMS) δ_H (ppm): 11.03 (s, 1H, –OH), 7.87 (s, 1H, –CH=N), 7.25–6.83 (m, 4H, ArH), 5.42 (s, 2H, $-NH_2$).

2.3.2 Synthesis of 4-n-nonyloxybenzaldehyde

To a solution of 4-hydroxybenzaldehyde (1.22 g, 10 mmol) in acetone (30 ml) were added 1-bromononane (1.9 ml, 10 mmol), K_2CO_3 (2.07g, 15 mmol) and KI (catalytic amount). The reaction mixture was refluxed for 24 h. The residue was filtered off and the solvent was removed from the filtrate under reduced pressure. The crude oil thus obtained was purified by distillation under reduced pressure. Yield: 83%, FT-IR (KBr, cm^{-1}): 2937, 2858 (aliphatic C–H), 1689 (C=O), 1602, 1510 (Ph), 1311, 1259 (OPh). ^1H NMR ($CDCl_3$, TMS) δ_H (ppm): 9.87 (s, 1H, –CHO), 7.84–6.88 (d, 4H, ArH), 4.06–4.01 (t, 2H, $-OCH_2$), 2.36–1.31 (m, 14H, $-[CH_2]_n$), 0.89 (t, 3H, CH_3).

All other members of the homologous series 4-hexyloxy-, heptyloxy-, octyloxy-, decyloxy-, undecyloxy-, dodecyloxy-, tetradecyloxy- and hexadecyloxy benzaldehydes were prepared using the above procedure.

2.3.3 Synthesis of N-(o-hydroxybenzylidene)-N′-(4-n-nonyloxybenzylidene)azine (3d)

To a solution of 4-nonyloxybenzaldehyde (1.24 g, 5 mmol) in chloroform (20 ml) was added 0.68 g (5 mmol) of salicylhydrazone, which was stirred at room temperature for 8 h. The yellow precipitate formed was filtered, washed with methanol (2 × 5 ml) and dried under reduced pressure.

All other members of the homologous series were prepared in a similar manner. The yield, IR, NMR and elemental data for the compounds are summarised as follows.

2.3.4 N-(o-hydroxybenzylidene)-N′-(4-n-hexyloxybenzylidene)azine, $C_{20}H_{24}N_2O_2$ (3a)

Yield: 62%. FT-IR (KBr, cm^{-1}): 3450 (OH), 2917, 2849 (aliphatic C–H), 1619 (C=N), 1573, 1469 (Ph), 1308, 1261 (OPh), 1020 (N–N). ^1H NMR ($CDCl_3$, TMS) δ_H (ppm): 11.81 (s, 1H, –OH), 8.71 (s, 1H, $-C_6H_4OHC\underline{H}{=}N$), 8.59 (s, 1H, $ROC_6H_4C\underline{H}{=}N$), 7.78–6.94 (m, 8H, ArH), 4.04–4.00 (t, 2H, $-OCH_2$),

Downloaded At: 14:08 25 January 2011

Downloaded At: 14:08 25 January 2011

1.83–1.34 (m, 8H, –$[CH_2]_n$), 0.93–0.89 (t, 3H, –CH_3). UV–visible ($CHCl_3$): λ_{max} = 390, 322, 262 nm. Elemental analyses: calculated for $C_{20}H_{24}N_2O_2$ (%), C, 74.04; H, 7.45; N, 8.63; Found, C, 74.28; H, 7.34; N, 8.70.

2.3.5 N-(o-hydroxybenzylidene)-N′-(4-n-heptyloxybenzylidene)azine, $C_{21}H_{26}N_2O_2$ ***(3b)***

Yield: 65%. FT-IR (KBr, cm^{-1}): 3448 (OH), 2928, 2858 (aliphatic C–H), 1620 (C=N), 1509, 1477 (Ph), 1306, 1250 (OPh), 1016 (N–N). ^{1}H NMR ($CDCl_3$, TMS) δ_H (ppm): 11.37 (s, 1H, –OH), 8.71 (s, 1H, –$C_6H_4OHC\underline{H}$=N), 8.59 (s, 1H, $ROC_6H_4C\underline{H}$=N), 7.77–6.92 (m, 8H, ArH), 4.02–3.98 (t, 2H, –OCH_2), 1.82–1.31 (m, 10H, –$[CH_2]_n$), 0.89 (t, 3H, –CH_3). UV–visible ($CHCl_3$): λ_{max} = 392, 353, 322, 283, 263 nm. Elemental analyses: calculated for $C_{21}H_{26}N_2O_2$ (%), C, 74.52; H, 7.44; N, 8.27; Found, C, 74.34; H, 7.12; N, 7.64.

2.3.6 N-(o-hydroxybenzylidene)-N′-(4-n-octyloxybenzylidene)azine, $C_{22}H_{28}N_2O_2$ ***(3c)***

Yield: 65%. FT-IR (KBr, cm^{-1}): 3451 (OH), 2922, 2855 (aliphatic C–H), 1621 (C=N), 1509, 1481 (Ph), 1308, 1254 (OPh), 1030 (N–N). ^{1}H NMR ($CDCl_3$, TMS) δ_H (ppm): 11.81 (s, 1H, –OH), 8.71 (s, 1H –$C_6H_4OHC\underline{H}$=N), 8.59 (s, 1H, $ROC_6H_4C\underline{H}$=N), 7.78–6.92 (m, 8H, ArH), 4.04–3.98 (t, 2H, –OCH_2), 1.82–1.30 (m, 12H, –$[CH_2]_n$), 0.90–0.87 (t, 3H, –CH_3). ^{13}C NMR δ_C ($CDCl_3$): 164.6, 163.9 (CH=N), 162.0, 161.5, 159.7 (C–OH), 132.5 (Ar–C), 130.4, 126.7, 125.9, 119.3, 117.8, 117.2, 116.9, 114.8, 114.7, 77.4, 77.0, 76.5 ($CDCl_3$), 68.1 (–OCH_2), 31.7, 29.3, 29.1, 25.9, 22.6, 14.0 (CH_3). UV–visible ($CHCl_3$): λ_{max} = 397, 353, 292, 261 nm. Elemental analyses: calculated for $C_{22}H_{28}N_2O_2$ (%), C, 74.96; H, 8.00; N, 7.94; Found, C, 74.54; H, 8.29; N, 7.62.

2.3.7 N-(o-hydroxybenzylidene)-N′-(4-n-nonyloxybenzylidene)azine, $C_{23}H_{30}N_2O_2$ ***(3d)***

Yield: 69%. FT-IR (KBr, cm^{-1}): 3427 (OH), 2937, 2864 (aliphatic C–H), 1616 (C=N), 1511, 1474 (Ph), 1308, 1249 (OPh), 1026 (N–N). ^{1}H NMR ($CDCl_3$, TMS) δ_H (ppm): 11.82 (s, 1H, –OH), 8.71 (s, 1H, –$C_6H_4OHC\underline{H}$=N), 8.59 (s, 1H, $ROC_6H_4C\underline{H}$=N), 7.78–6.94 (m, 8H, ArH), 4.03–4.00 (t, 2H, –OCH_2) 1.83–1.28 (m, 14H, –$[CH_2]_n$), 0.90–0.86 (t, 3H, –CH_3). ^{13}C NMR δ_C ($CDCl_3$): 164.6, 163.9 (CH=N), 162.0, 161.5, 159.7 (C–OH), 132.5 (Ar–C), 130.4, 126.7, 125.9, 119.3, 117.8, 117.2, 116.8, 114.8, 114.7, 77.4, 77.0, 76.5 ($CDCl_3$), 68.1 (–OCH_2), 31.8, 29.4, 29.3, 29.1, 25.9, 22.6, 14.0 (CH_3). UV–visible ($CHCl_3$): λ_{max} = 389, 306, 261 nm. Elemental analyses: calculated for $C_{23}H_{30}N_2O_2$ (%), C, 75.37; H, 8.25; N, 7.64; Found, C, 75.72; H, 7.92; N, 7.15.

2.3.8 N-(o-hydroxybenzylidene)-N′-(4-n-decyloxybenzylidene)azine, $C_{24}H_{32}N_2O_2$ ***(3e)***

Yield: 72%. FT-IR (KBr, cm^{-1}): 3449 (OH), 2921, 2853 (aliphatic C–H), 1615 (C=N), 1509, 1469 (Ph), 1307, 1258 (OPh), 1011 (N–N). ^{1}H NMR ($CDCl_3$, TMS) δ_H (ppm): 11.81 (s, 1H, –OH), 8.73 (s, 1H, –$C_6H_4OHC\underline{H}$=N), 8.59 (s, 1H, $ROC_6H_4C\underline{H}$=N), 7.78-6.94 (m, 8H, ArH), 4.04–4.00 (t, 2H, –OCH_2), 1.83–1.34 (m, 16H, –$[CH_2]_n$), 0.93–0.89 (t, 3H, –CH_3). UV–visible ($CHCl_3$): λ_{max} = 380, 354, 318, 281, 262 nm. Elemental analyses: calculated for $C_{24}H_{32}N_2O_2$ (%), C, 75.75; H, 8.47; N, 7.36; Found, C, 75.36; H, 8.42; N, 7.54.

2.3.9 N-(o-hydroxybenzylidene)-N′-(4-n-undecyloxybenzylidene)azine, $C_{25}H_{34}N_2O_2$ ***(3f)***

Yield: 73%. FT-IR (KBr, cm^{-1}): 3452 (OH), 2921, 2851 (aliphatic C–H), 1619 (C=N), 1512, 1481 (Ph), 1307, 1267 (OPh), 1024 (N–N). ^{1}H NMR ($CDCl_3$, TMS) δ_H (ppm): 11.81 (s, 1H, –OH), 8.73 (s, 1H, –$C_6H_4OHC\underline{H}$=N), 8.59 (s, 1H, $ROC_6H_4C\underline{H}$=N), 7.78–6.91 (m, 8H, ArH), 4.03–3.84 (t, 2H, –OCH_2), 1.83–1.27 (m, 18H, –$[CH_2]_n$), 0.90–0.86 (t, 3H, –CH_3). ^{13}C NMR δ_C ($CDCl_3$): 164.6, 163.9 (CH=N), 162.0, 161.5, 159.7 (C–OH), 132.5 (Ar–C), 130.3, 126.7, 126.0, 119.3, 117.8, 117.2, 117.1, 116.8, 114.8, 114.6, 77.4, 77.0, 76.5 ($CDCl_3$), 68.1 (–OCH_2), 31.8, 29.6, 29.5, 29.3, 29.1, 25.9, 22.6, 14.0 (CH_3). UV–visible: λ_{max} = 391, 353, 324, 297, 259, 211 nm. Elemental analyses: calculated for $C_{25}H_{34}N_2O_2$ (%), C, 76.10; H, 8.68; N, 7.10; Found C, 75.92; H, 8.50; N, 6.94.

2.3.10 N-(o-hydroxybenzylidene)-N′-(4-n-dodecyloxybenzylidene)azine, $C_{26}H_{36}N_2O_2$ ***(3g)***

Yield: 76%. FT-IR (KBr, cm^{-1}): 3447 (OH), 2921, 2852 (aliphatic C–H), 1618 (C=N), 1509, 1473 (Ph), 1307, 1249 (OPh), 1024 (N–N). ^{1}H NMR ($CDCl_3$, TMS) δ_H (ppm): 11.82 (s, 1H, –OH), 8.71 (s, 1H, –$C_6H_4OHC\underline{H}$=N), 8.59 (s, 1H, $ROC_6H_4C\underline{H}$=N), 7.78–6.94 (m, 8H, ArH), 4.03-4.00 (t, 2H, –OCH_2), 1.82–1.26 (m, 20H, –$[CH_2]_n$), 0.90–0.86 (t, 3H, –CH_3). ^{13}C NMR δ_C ($CDCl_3$): 164.6, 163.9 (CH=N), 162.0, 161.5, 159.7 (C–OH), 132.5 (Ar–C), 130.3, 126.7, 125.9, 119.3, 117.8, 117.2, 117.1, 116.8, 114.8, 114.6, 77.4, 77.0, 76.5 ($CDCl_3$), 68.1 (–OCH_2), 31.8, 29.6, 29.5, 29.3, 25.9, 22.6, 14.0 (CH_3). UV–visible ($CHCl_3$): λ_{max} = 387, 301, 262 nm. Elemental analyses: calculated for $C_{26}H_{36}N_2O_2$ (%), C, 76.43; H, 8.88; N, 6.85; Found C, 76.84; H, 8.64; N, 6.54.

2.3.11 N-(o-hydroxybenzylidene)-N′-(4-n-tetradecyloxybenzylidene)azine, $C_{28}H_{40}N_2O_2$ ***(3h)***

Yield: 77%. FT-IR (KBr, cm^{-1}): 3508 (OH), 2920, 2850 (aliphatic C–H), 1617 (C=N), 1510, 1473 (Ph),

1308, 1251 (OPh), 1020 (N–N). ^{1}H NMR ($CDCl_3$, TMS) δ_H (ppm): 11.81 (s, 1H, –OH), 8.71 (s, 1H, $-C_6H_4OHC\underline{H}=N$), 8.59 (s, 1H, $ROC_6H_4C\underline{H}=N$), 7.78–6.94 (m, 8H, ArH), 4.03–3.98 (t, 2H, $-OCH_2$), 1.82–1.26 (m, 24H, $-[CH_2]_n$), 0.90–0.85 (t, 3H, $-CH_3$). UV–visible ($CHCl_3$): λ_{max} = 390, 323, 306, 263 nm. Elemental analyses: calculated for $C_{28}H_{40}N_2O_2$ (%), C, 77.02; H, 9.23; N, 6.41; Found, C, 77.28; H, 8.90; N, 6.34.

2.3.12 N-(o-hydroxybenzylidene)-N′-(4-n-hexadecyloxybenzylidene)azine, $C_{30}H_{44}N_2O_2$ (3i)

Yield: 78%. FT-IR (KBr, cm^{-1}): 3508 (OH), 2918, 2849 (aliphatic C–H), 1620 (C=N), 1514, 1470 (Ph), 1309, 1262 (OPh), 1023 (N–N). ^{1}H NMR ($CDCl_3$, TMS) δ_H (ppm): 11.81 (s, 1H, –OH), 8.71 (s, 1H, $-C_6H_4OHC\underline{H}=N$), 8.59 (s, 1H, $ROC_6H_4C\underline{H}=N$), 7.78–6.94 (m, 8H, ArH), 4.03–4.00 (t, 2H, $-OCH_2$), 1.82–1.26 (m, 28H, $-[CH_2]_n$), 0.89–0.85 (t, 3H, $-CH_3$). UV–visible ($CHCl_3$): λ_{max} = 383, 311, 267 nm. Elemental analyses: calculated for $C_{30}H_{44}N_2O_2$ (%), C, 77.54; H, 9.54; N, 6.02; Found, C, 77.37; H, 9.16; N, 5.98.

3. Synthesis of copper (II) complex of N-(*o*-hydroxybenzylidene)-N′-(4-n-nonyloxybenzylidene)azine (4)

To a solution of N-(*o*-hydroxybenzylidene)-N′-(4-n-nonyloxy benzylidene)azine (1.46 g, 4 mmol) in chloroform (20 ml) was added a solution of copper (II) acetate (0.39 g, 2 mmol) in methanol (20 ml); a brown precipitate started to appear. The reaction mixture was stirred at room temperature for 1 h to complete the reaction. The precipitate was filtered off and washed with chloroform and methanol thrice each.

The copper (II) complexes of all azines were prepared following the above procedure. These compounds were characterised by IR light, NMR, UV–visible spectroscopy, ESR, the magnetic moment and analytical data, which are summarised below.

3.1 Bis[N-(o-hydroxybenzylidene)-N′-(4-n-hexyloxybenzylidene)azine] copper (II) complex, $C_{40}H_{46}N_4O_4Cu$ (4a)

Brown, yield: 47%. FT-IR (KBr, cm^{-1}): 2932, 2860 (aliphatic C–H), 1610 (C=N), 1515 (Ph), 1245 (OPh), 1025 (N–N). Far IR (nujol): 478, 382, 186, 127, 79 cm^{-1}. ^{1}H NMR ($CDCl_3$ TMS) δH (ppm): 8.59 (s, 4H, CH=N), 7.78–6.94 (m, 16H, ArH), 4.02–4.00 (t, 4H, $-OCH_2$), 1.80–1.31(m, 16H, $-[CH_2]_n$), 0.89(t, 6H, $-CH_3$). UV–visible (nujol): λ_{max} = 397, 325, 255 nm. μ_{eff}: 2.08 BM. Elemental analyses: calculated for $C_{40}H_{46}N_4O_4Cu$ (%), C, 67.63; H, 6.52; N, 7.88; Cu, 8.94 Found, C, 67.25; H, 6.18; N, 7.15; Cu, 8.67.

3.1.1 Bis[N-(o-hydroxybenzylidene)-N′-(4-n-heptyloxybenzylidene)azine] copper (II) complex, $C_{42}H_{50}N_4O_4Cu$ (4b)

Brown, yield: 44%. FT-IR (KBr, cm^{-1}): 2928, 2858 (aliphatic C–H), 1610 (C=N), 1513 (Ph), 1247 (OPh), 1011 (N–N). Far IR (nujol): 552, 507, 474, 392, 353, 277, 213, 151, 106 cm^{-1}. ^{1}H NMR ($CDCl_3$ TMS) δH (ppm): 8.60 (s, 4H, CH=N), 7.77–6.93 (m, 16H, ArH), 4.02–4.00 (t, 4H, $-OCH_2$), 1.79–1.25 (m, 20H, $-[CH_2]_n$) 0.88 (t, 6H, $-CH_3$). UV–visible (nujol): λ_{max} = 417, 327, 304, 247 nm. μ_{eff}: 2.03 BM. Elemental analyses: calculated for $C_{42}H_{50}N_4O_4Cu$ (%), C, 68.31; H, 6.82; N, 7.58; Cu, 8.60; Found, C, 68.12; H, 6.43; N, 7.34; Cu, 8.32.

3.1.2 Bis[N-(o-hydroxybenzylidene)-N′-(4-n-octyloxybenzylidene)azine] copper (II) complex, $C_{44}H_{54}N_4O_4Cu$ (4c)

Brown, yield: 52%. FT-IR (KBr, cm^{-1}): 2923, 2855 (aliphatic C–H), 1609 (C=N), 1513 (Ph), 1250 (OPh), 1029 (N–N). Far IR (nujol): 461, 364, 149, 97 cm^{-1}. ^{1}H NMR ($CDCl_3$ TMS) δH (ppm): 8.59 (s, 4H, CH=N), 7.77–6.93 (m, 16H, ArH), 4.02–4.00 (t, 4H, $-OCH_2$), 1.80–1.31 (m, 24H, $-[CH_2]_n$) 0.89 (t, 6H, $-CH_3$). UV–visible (nujol): λ_{max} = 445, 327, 251 nm. μ_{eff} 1.72 BM. Elemental analyses: calculated for $C_{44}H_{54}N_4O_4Cu$ (%), C, 68.94; H, 7.10; N, 7.30; Cu, 8.29; Found, C, 68.52; H, 7.12; N, 7.24; Cu, 8.15.

3.1.3 Bis[N-(o-hydroxybenzylidene)-N′-(4-n-nonyloxybenzylidene)azine] copper (II) complex, $C_{46}H_{58}N_4O_4Cu$ (4d)

Brown, yield: 54%. FT-IR (KBr, cm^{-1}): 2919, 2851 (aliphatic C–H), 1607 (C=N), 1512 (Ph), 1253 (OPh), 1038 (N–N). Far IR (nujol): 538, 461, 349, 269, 152 cm^{-1}. ^{1}H NMR ($CDCl_3$ TMS) δH (ppm):8.59 (s, 4H, CH=N), 7.77–6.93 (m, 16H, ArH), 4.02–4.00 (t, 4H, $-OCH_2$), 1.80–1.31 (m, 28H, $-[CH_2]_n$) 0.89 (t, 6H, $-CH_3$). UV–visible (nujol): λ_{max} = 418, 378, 327, 304, 249 nm. μ_{eff}: 1.75 BM. Elemental analyses: calculated for $C_{46}H_{58}N_4O_4Cu$ (%), C, 69.53; H, 7.35; N, 7.05; Cu, 7.99; Found, C, 69.81; H, 7.24; N, 7.01; Cu, 7.62.

3.1.4 Bis[N-(o-hydroxybenzylidene)-N′-(4-n-decyloxybenzylidene)azine] copper (II) complex, $C_{48}H_{62}N_4O_4Cu$ (4d)

Brown, yield: 57%. FT-IR (KBr, cm^{-1}): 2919, 2851 (aliphatic C–H), 1607 (C=N), 1512 (Ph), 1254 (OPh), 1038 (N–N). Far IR (nujol): 470, 419, 353, 133 cm^{-1}. ^{1}HNMR ($CDCl_3$ TMS) δH (ppm): 8.59 (s, 4H, –CH=N), 7.72–6.92 (m, 16H, ArH), 4.02–4.00 (t, 4H, $-OCH_2$), 1.83–1.31 (m, 32H, $-[CH_2]_n$) 0.89

Downloaded At: 14:08 25 January 2011

(t, 6H, $-CH_3$). UV–visible (nujol): λ_{max} = 380, 354, 318, 281, 262 nm. μ_{eff}: 1.80 BM. Elemental analyses: calculated for $C_{48}H_{62}N_4O_4Cu$ (%), C, 70.08; H, 7.59; N, 6.81; Cu, 7.72; Found, C, 70.15; H, 7.92; N, 6.56; Cu, 7.68.

3.1.5 Bis[N-(o-hydroxybenzylidene)-N′-(4-n-undecyloxybenzylidene)azine]copper (II) complex, $C_{50}H_{66}N_4O_4Cu$ ***(4f)***

Brown, yield: 58%. FT-IR (KBr, cm^{-1}): 2918, 2851 (aliphatic C–H), 1610 (C=N), 1511 (Ph), 1248 (OPh), 1025 (N–N). Far IR (nujol): 475, 394, 339, 200, 153, 95 cm^{-1}. ^{1}H NMR ($CDCl_3$ TMS) δH (ppm): 8.59 (s, 4H, –CH=N), 7.77–6.92 (m, 16H, ArH), 4.02–4.00 (t, 4H, $-OCH_2$), 1.80–1.31 (m, 36H, $-[CH_2]_n$) 0.89 (t, 6H, $-CH_3$). UV–visible: (nujol): λ_{max} = 318, 251, 223 nm. μ_{eff}: 1.88 BM. Elemental analyses: for $C_{50}H_{66}N_4O_4Cu$ (%), C, 70.59; H, 7.82; N, 6.58; Cu, 7.47; Found, C, 70.54; H, 7.58; N, 6.92; Cu, 7.34.

3.1.6 Bis[N-(o-hydroxybenzylidene)-N′-(4-n-dodecyloxybenzylidene)azine]copper (II) complex, $C_{52}H_{70}N_4O_4Cu$ ***(4g)***

Brown, yield: 65%. FT-IR (KBr, cm^{-1}): 2920, 2851 (aliphatic C–H), 1612 (C=N), 1512 (Ph), 1251 (OPh), 1033 (N–N). Far IR (nujol): 489, 383, 304, 148, 97 cm^{-1}. ^{1}H NMR ($CDCl_3$ TMS) δH (ppm): 8.59 (s, 4H, –CH=N), 7.77-6.92 (m, 16H, ArH), 4.02–4.00 (t, 4H, $-OCH_2$), 1.80–1.31 (m, 40H, $-[CH_2]_n$) 0.89 (t, 6H, $-CH_3$). UV–visible (nujol): λ_{max} = 391, 341, 314, 246, 218 nm. μ_{eff}: 1.85 BM. Elemental analyses: calculated for $C_{52}H_{70}N_4O_4Cu$ (%), C, 71.07; H, 8.02; N, 6.37; Cu, 7.23; Found, C, 70.94; H, 7.66; N, 6.52; Cu, 7.43.

3.1.7 Bis[N-(o-hydroxybenzylidene)-N′-(4-n-tetradecyloxybenzylidene)azine]copper (II) complex, $C_{56}H_{78}N_4O_4Cu$ ***(4h)***

Brown, yield: 67%. FT-IR (KBr, cm^{-1}): 2920, 2853 (aliphatic C–H), 1611 (C=N), 1512 (Ph), 1252 (OPh), 1037 (N–N). Far IR (nujol): 477, 436, 387, 329, 151, 83cm^{-1}. ^{1}H NMR ($CDCl_3$ TMS) δH (ppm): 8.59 (s, 4H, –CH=N), 7.77–6.92 (m, 16H, ArH), 4.02–4.00 (t, 4H, $-OCH_2$), 1.80–1.31 (m, 48H, $-[CH_2]_n$) 0.89 (t, 6H, $-CH_3$). UV–visible (nujol): λ_{max} = 304, 247, 224 nm. μ_{eff}: 1.78 BM. Elemental analyses: calculated for $C_{56}H_{78}N_4O_4Cu$ (%), C, 71.95; H, 8.40; N, 5.99; Cu, 6.79; Found, C, 71.72; H, 8.36; N, 5.42; Cu, 6.76.

3.1.8 Bis[N-(o-hydroxybenzylidene)-N′-(4-n-hexadecyloxybenzylidene)azine]copper (II) complex, $C_{60}H_{86}N_4O_4Cu$ ***(4i)***

Brown, yield: 64%. FT-IR (KBr, cm^{-1}): 2919, 2852 (aliphatic C–H), 1609 (C=N), 1512 (Ph), 1252 (OPh), 1042 (N–N). Far IR (nujol): 432, 388, 195, 114 cm^{-1}. ^{1}H NMR ($CDCl_3$ TMS) δH (ppm):8.59 (s, 4H, –CH=N), 7.77–6.92 (m, 16H, ArH), 4.02–4.00 (t, 4H, $-OCH_2$), 1.80–1.31 (m, 56H, $-[CH_2]_n$) 0.89 (t, 6H, $-CH_3$). UV–visible (nujol): λ_{max} = 395, 351, 305, 266, 237 nm. μ_{eff}: 1.70 BM. Elemental analyses: calculated for $C_{60}H_{86}N_4O_4Cu$ (%), C, 72.72; H, 8.74; N, 5.65; Cu, 6.41; Found, C, 72.54; H, 8.37; N, 5.61; Cu, 6.52.

4. Results and discussion

The synthetic route for the preparation of the compounds N-(*o*-hydroxy benzylidene)-N′-(4-n-alkoxybenzylidene)azines **3a–i** and their copper (II) complexes **4a–i** are outlined in Scheme 1. The elemental analyses, FT-IR and NMR spectra are fully consistent with the structure. The absorption bands appearing at 3481, 3383, 3287, 1617, 1573 and 1028 cm^{-1} in the FT-IR spectrum of salicylhydrazone (Figure 1) are attributed to ν(OH), ν_a(N–H), ν_s(N–H), ν(C=N), ν(Ph) and ν(N–N), respectively. In the spectrum of N-(*o*-hydroxybenzylidene)-N′-(4-n-nonyloxybenzylidene)azine **3d** (Figure 2) bands appearing at 3427, (2937, 2864), 1616, (1511, 1474), (1308, 1249) and 1026 cm^{-1} are assigned to the ν(OH), ν(aliphatic C–H), ν(C=N), ν(Ph), ν(OPh) and ν(N–N) modes, respectively. In the spectrum of the copper complex of N-(*o*-hydroxybenzylidene)-N′-(4-n-nonyloxybenzylidene)azine **4d** (Figure 3) the ν(C=N) bands shift to a lower frequency (1607 cm^{-1}), indicating bonding through azomethine nitrogen. The lowering in the ν(C=N) band caused by the coordination of nitrogen to the metal centre is in agreement with the result obtained for similar other complexes [29–33]. The bonding through nitrogen of the azine to the Cu(II) ion is further supported by the shift of ν(N–N) band to a higher position (1038 cm^{-1}) compared to its position in the spectrum of the parent ligand **3d** at 1026 cm^{-1}. The increase in frequency of the ν(N–N) band in the metal complex is due to decrease in repulsion between the lone pair of electrons on both the nitrogens. The far IR spectrum of **4d** shows the appearance of ν(M–N) and ν(M–O) bands at 461 and 349 cm^{-1}, which are evidence for the bonding of the azine to the copper(II).

The proton NMR spectrum of N-(*o*-hydroxybenzylidene)-N′-(4-n-nonyloxybenzylidene) azine **3d** (Figure 4) exhibits peaks at δ 11.82(s), 8.71(s), 8.59(s), 7.78–6.94, 4.03–4.00, 1.83–1.28 and 0.90-0.86, which are attributed to –OH and CH=N of ortho hydroxybenzylidene and CH=N of para alkoxybenzylidene, ring, $-OCH_2$, $-[CH_2]_n$ and $-CH_3$ protons, respectively. The spectrum of the bis[N-(*o*-hydroxybenzylidene)-N′-(4-n-nonyloxybenzylidene)azine] copper(II) **4d** (Figure 5) complex reveals peaks at δ 8.59, 7.77–6.93, 4.02–4.00, 1.80–1.31 and 0.89, which are attributed to CH=N, ring, $-OCH_2$, $-[CH_2]_n$ and $-CH_3$ protons,

Downloaded At: 14:08 25 January 2011

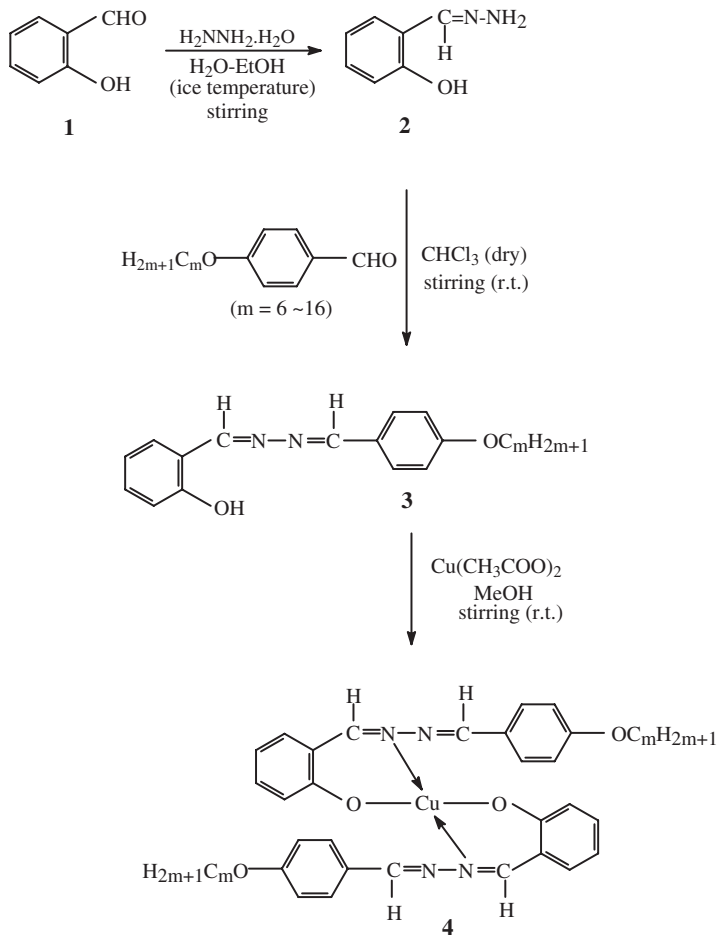

Scheme 1. Route for the synthesis of N-(*o*-hydroxybenzylidene)-N′-(4-n-alkoxy benzylidene)azines and their copper (II) complexes.

Downloaded At: 14:08 25 January 2011

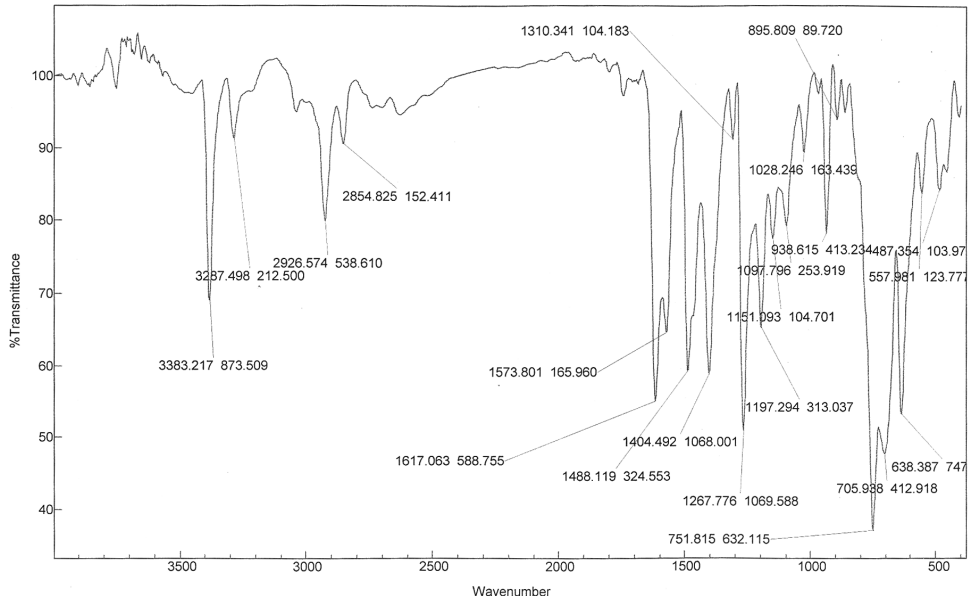

Figure 1. FT-IR spectrum of salicylhydrazone.

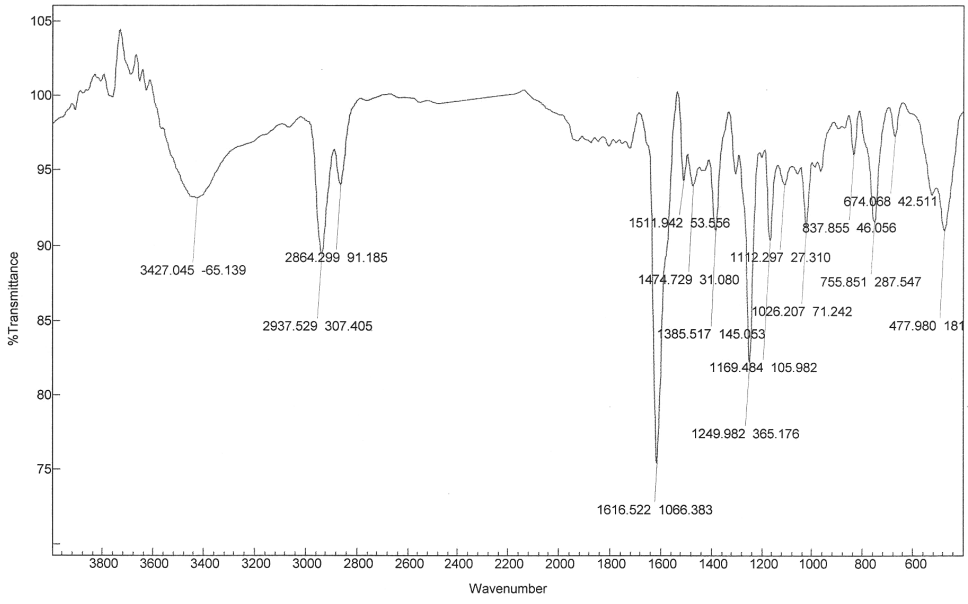

Figure 2. FT-IR spectrum of N-(*o*-hydroxybenzylidene)-N′-(4-n-nonyloxybenzylidene)azine **3d**.

Downloaded At: 14:08 25 January 2011

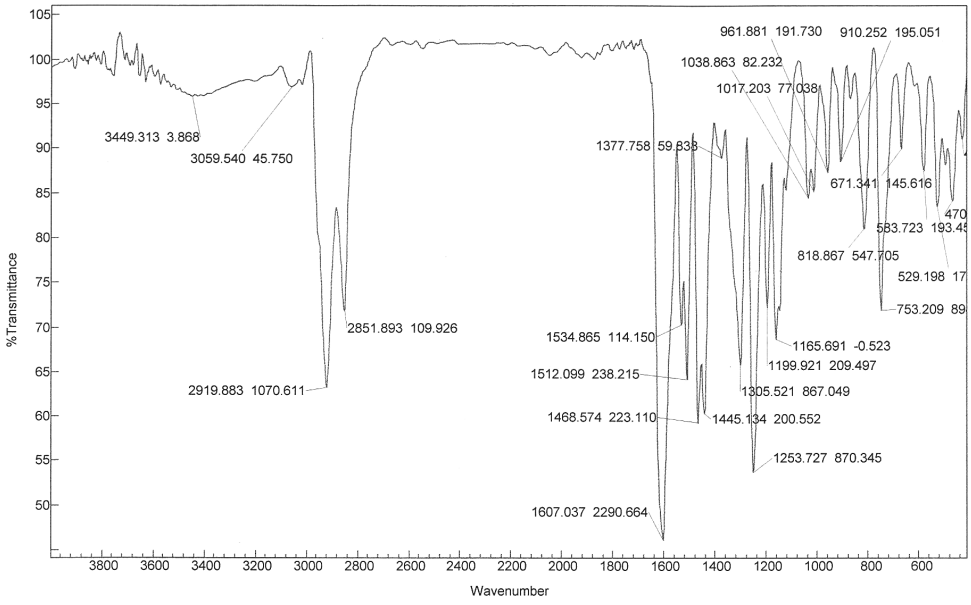

Figure 3. FT-IR spectrum of bis[N-(*o*-hydroxybenzylidene)-N′-(4-n-nonyloxybenzylidene)azine] copper (II) complex **4d**.

respectively. The disappearance of the –OH signal from the spectrum of the metal complex indicates that the OH group has been deprotonated and the resulting phenolate oxygen is bonded to the metal. The bonding of one of the azomethine nitrogens in proximity to the phenoxy oxygen would result in a downfield shift in the CH=N signal and thus giving one signal at higher positions than that in the free azine and one signal due to the CH=N of alkoxy azine. However, only one signal is observed at the upfield (δ 8.60). The downfield shift in CH=N near copper may be counterbalanced by the upfield shift in the signal due to the delocalisation of the unpaired d-electron in the chelate ring. Thus only one signal is observed due to both types of CH=N protons. Owing to the presence of the unpaired electron it is expected that the proton signal would be broad. However, the lines are much sharper than expected (compound **4d,** Figure 5) in some of the copper (II) complexes. This may be reasoned as follows. The proton NMR signals from the copper (II) complex **4d**, having an unpaired electron, are unexpectedly sharp. Probably,

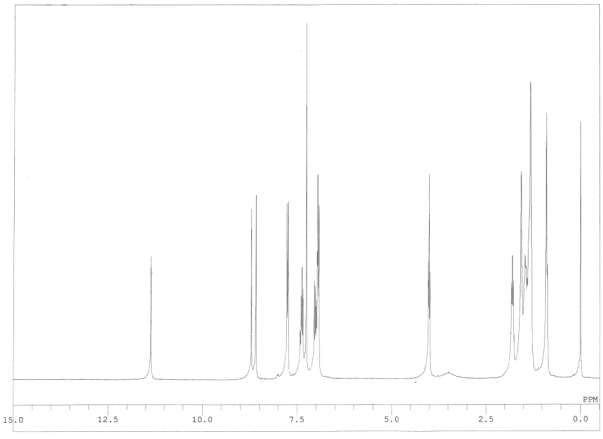

Figure 4. Proton NMR spectrum of N-(*o*-hydroxybenzylidene)-N′-(4-n-nonyloxybenzylidene)azine **3d**.

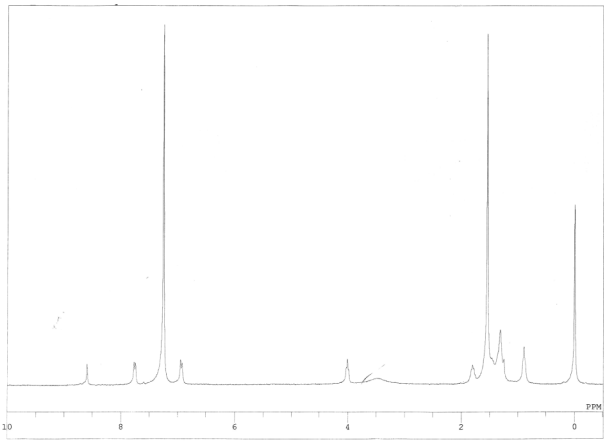

Figure 5. Proton NMR spectrum of bis[N-(*o*-hydroxybenzylidene)-N′-(4-n-nonyloxybenzylidene)azine] copper (II) complex **4d**.

the electron relaxation time for the complex is sufficiently larger than the hyperfine coupling constant (A) [34]. Sharp proton signals from other paramagnetic complexes, for example nickel aminotroponeiminates, have been reported [35]. Based on these observations and elemental data, it is concluded that the unsymmetrical azine is bonded to the metal ion as a bidentate (N, O) ligand.

The bands observed at 389, 306 and 261 nm in the electronic spectrum of N-(*o*-hydroxybenzylidene)-N′-(4-n-nonyloxybenzylidene)azine **3d** are assigned to n–π* and π–π* transitions. In the spectrum of the bis[N-(*o*-hydroxybenzylidene)-N′-(4-n-nonyloxybenzylidene)azine]copper (II) complex **4d** the bands are observed at 418, 378, 327, 304 and 249 nm. The first band is characteristic of square planar coordination around the metal centre [36]. The remaining bands are attributed to the π–π* and n–π* transitions of the ligand. The copper compounds exhibit magnetic moments at 1.70–2.08 BM, suggesting the presence of one unpaired electron. The ESR spectrum of N-(o-hydroxybenzylidene)-Ń-(4-n-alkoxybenzylidene)azine] copper(II)complex **4d** is not resolved. It gives lines at 2950 G in the parallel regions and at 3210 G in the perpendicular regions. These signals yield $g_{\|}$ (2.206) and $g_{\perp}$ (2.027). The g values are consistent with the square planar geometry around Cu (II) and the presence of an unpaired electron in the dx^2–y^2 orbital of the metal ion [37–40].

5. Optical properties

The liquid crystalline properties of N-(*o*-hydroxybenzylidene)-N′-(4-n-alkoxybenzylidene)azines **3a–i** and their copper (II) complexes were investigated by polarising optical microscopy using a heating and cooling stage. The phase transition temperatures and enthalpies were measured by carrying out DSC thermal analysis. The phase transition temperatures, enthalpy and entropy values for the azines and some of their copper complexes are summarised in Tables 1 and 2, respectively. The symbols K, SmA, N and I denote crystalline, SmA, nematic and isotropic phases, respectively. The compound **3c** showed endothermic peaks at 76.5, 95.3, 102.7 and 164.2°C followed by the appearance of exothermic peaks at 117.3, 100.3 and 92.6°C. The three endothermic peaks observed for this compound define the crystal-to-crystal phase transition and the fourth peak defines the crystal-to-isotropic phase transition. The exothermic peaks reveal an isotropic-to-mesophase transition and a mesophase-to-crystal phase followed by the next crystal phase in the cooling cycle. A salient monotropic nematic phase with a schlieren texture (Figure 6) is revealed for this compound in the cooling cycle on the basis of polarising optical microscopy. The two to four black brushes (black stripes) seen emerging from the central nuclei are generally line defects that form disclination lines and are observed as long black stripes in the nematic phase exclusively for this compound. This nematic phase appears as nematic droplets with a schlieren texture as seen under optical microscopy at 117.3°C in the cooling cycle. These droplets start to appear from the border limit of the sample and a sudden phase transition at 100.3°C leads to the appearance of the crystal phase. Compound **3a** exhibits peaks in the heating cycle at 210.0 due to the crystal-to-isotropic transition. However, it exhibits exothermic peaks at 141.3 and 100.3°C involving enthalpies 0.04 and 6.4 kJ mol^{-1} and accompanied by entropies 0.09 and 17.2 JK^{-1} mol^{-1}. This defines the isotropic-to-mesophase and the mesophase-to-crystal phase transitions, respectively. The texture of the mesophase revealed

Downloaded At: 14:08 25 January 2011

Table 1. Transition temperature (T), transition enthalpy (ΔH) and transition entropy (ΔS) of N-(*o*-hydroxybenzylidene)-N′-(4-n-alkoxybenzylidene)azine.

Compounds	Transitions	T (°C)	ΔH (kJ mol^{-1})	ΔS (J K^{-1} mol^{-1})
3a	K–I	210.0	41.9	86.8
	I–SmA	141.3	0.04	0.09
	SmA–K	100.3	6.4	17.2
3b	K^1–K^2	65.0	10.2	30.1
	K^2–K^3	128.7	19.6	48.7
	K^3–I	164.7	14.0	32.0
	I–K	112.2	11.0	28.5
3c	K^1–K^2	76.5	14.5	41.4
	K^2–K^3	95.3	2.4	6.5
	K^3–K^4	102.7	1.4	3.8
	K^4–I	164.2	4.4	10.0
	I–N	117.3	15.4	39.4
	N–K^3	100.3	0.2	0.5
	K^3–K	92.6	4.0	10.9
3d	K^1–I	60.4	17.8	53.4
	I–SmA	70.9	1.7	5.0
	SmA–K	60.0	10.7	32.1
3e	K^1–K^2	65.0	0.1	0.2
	K^2–I	86.2	38.4	106.9
	I–SmA	54.3	0.5	1.6
	SmA–K	39.7	18.5	59.2
3f	K^1–K^2	66.9	24.6	72.3
	K^2–K^3	76.7	1.1	3.2
	K^3–I	84.8	5.5	15.3
	I–SmA	65.9	1.6	4.8
	SmA–K	61.3	3.4	10.1
3g	K^1–K^2	67.8	27.2	79.8
	K^2–I	77.7	1.4	4.0
	I–SmA	85.1	6.4	17.8
	SmA–K	59.7	15.7	47.1
3h	K^1–K^2	73.8	22.8	65.7
	K^2–I	93.1	10.0	27.3
	I–SmA	82.7	5.7	16.0
	SmA–K	58.2	10.8	32.6
3i	K^1–K^2	70.0	35.1	102.3
	K^2–I	91.6	8.8	24.2
	I–SmA	74.8	17.1	49.1
	SmA–K	34.9	14.9	48.3

Table 2. Transition temperature (T), transition enthalpy (ΔH) and transition entropy (ΔS) of bis[N-(*o*-hydroxybenzylidene)-N′-(4-n-alkoxybenzylidene)azine] copper (II) complexes.

Compounds	Transitions	T (°C)	ΔH (kJ mol^{-1})	ΔS (J K^{-1} mol^{-1})
4a	K^1–K^2	64.8	0.2	0.6
	K^2–K^3	102.6	13.2	35.1
	K^3–K^4	145.8	0.4	0.9
	K^4–I	187.2	0.08	0.1
	I–K^4	182.6	0.2	0.4
	K^4–K^3	141.3	0.4	1.0
	K^3–K^2	100.3	0.6	1.6
	K^2–K^1	76.8	2.3	6.6
	K^1–$K^{"}$	70.6	1.5	4.3
	$K^{"}$–K	57.3	0.5	1.5
4c	K^1–K^2	65.5	0.5	1.4
	K^2–K^3	93.0	9.7	26.6
	K^3–K^4	105.0	0.3	0.8
	K^4–K^5	114.3	5.5	14.2
	K^5–K^6	145.8	0.3	0.7
	K^6–I	187.3	0.2	0.4
	I–K^6	182.5	0.3	0.6
	K^6–K^5	141.1	0.7	1.6
	K^5–K^4	104.5	6.2	16.4
	K^4–K^3	100.3	0.8	2.2
	K^3–K	57.4	0.7	2.2
4f	K^1–K^2	56.0	12.0	36.4
	K^2–K^3	65.0	0.5	1.4
	K^3–K^4	75.8	2.7	7.7
	K^4–K^5	105.1	0.4	1.0
	K^5–K^6	146.0	0.3	0.7
	K^6–I	187.1	0.3	0.6
	I–K^6	182.6	0.5	1.0
	K^6–K^5	141.1	0.8	1.9
	K^5–K^4	100.3	1.2	3.2
	K^4–K	56.9	0.8	2.4
4g	K^1–K^2	65.0	1.1	3.2
	K^2–K^3	94.9	12.2	33.1
	K^3–K^4	103.2	25.6	68.1
	K^4–K^5	146.0	0.5	1.2
	K^5–I	182.5	0.5	1.0
	I–K^5	141.1	0.8	2.0
	K^5–K^4	100.3	1.5	4.0
	K^4–K^3	89.5	12.8	35.4
	K^3–K^2	84.9	20.1	56.1
	K^2–K^1	72.6	9.0	26.0
	K^1–K	57.1	1.3	3.9
4i	K^1–K^2	64.3	0.6	1.7
	K^2–K^3	86.0	11.1	30.9
	K^3–K^4	104.6	0.6	1.5
	K^4–K^5	145.4	0.7	1.6
	K^5–I	186.8	0.2	0.4
	I–K^5	183.1	0.4	0.8
	K^5–K^4	141.7	0.7	1.6
	K^4–K^3	100.9	1.1	2.9
	K^3–K^2	73.0	5.4	15.7
	K^2–K^1	60.5	1.9	5.6

under the polarising microscope is characteristic of a SmA mesophase, having a fluid property with higher viscosity and having stratified structures with well-defined interlayer spacings. The interlayer attractions are weak and the layers are able to slide over one another relatively easily. The flexibility of the layers leads to distortions, which give rise to beautiful optical patterns known as the focal-conic texture (Figure 7). The molecules are aligned parallel to the layer normal, maintaining long-range orientational ordering and short-range positional ordering, which lead to the SmA mesophase. The molecular packings are found

Downloaded At: 14:08 25 January 2011

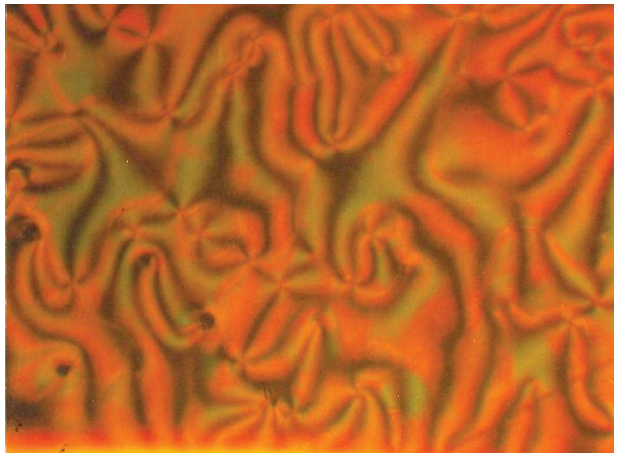

Figure 6. Photomicrograph of the nematic phase, with a schlieren texture, of compound **3c** at 117.3°C in the cooling cycle.

Figure 7. Photomicrograph of the SmA phase, with a focal-conic texture, of compound **3a** at 141.3°C in the cooling cycle.

Downloaded At: 14:08 25 January 2011

to be random for this SmA phase. The appearance of the SmA phase may arise due to the additional intramolecular forces between the phenolic OH group and the nitrogen atom in the unsymmetrical azines. Thus, a hexagonal pattern with a focal-conic texture is seen for this compound under optical microscopy, which confirms the SmA mesophase. A similar phase transition with a similar textural pattern is shown by compound **3d**. Compound **3e** shows endothermic peaks at 65.0 and 86.2°C having enthalpies at 0.1, 38.4 kJ mol^{-1}, signifying crystal-to-crystal and crystal-to-isotropic phase transitions, whereas the exothermic peaks appearing at 54.3 and 39.7 confer the isotropic-to-SmA and SmA-to-crystal phase transitions. Compound **3f** shows endothermic peaks at 66.9, 76.7 and 84.8 with enthalpy changes at 24.6, 1.1 and 5.5 kJ mol^{-1} and entropy changes of 72.3, 3.2 and 15.3 J K^{-1} mol^{-1}. The exothermic peaks are observed at 65.9 and 61.3°C. Polymorphism, based on the crystal-to-crystal phase transitions, is exhibited for this compound in the heating cycle and a monotropic SmA mesophase is observed at 65.9°C. The SmA mesophase transits to a crystal phase at 61.3°C. Thus, a monotropic nature is identified for this compound with the appearance of a SmA phase only in the cooling cycle. Compound **3g** shows crystal-to-crystal and crystal-to-isotropic phase transitions at 67.8 and 77.7°C. In the cooling cycle, the SmA phase appears at 85.1°C, followed by the appearance of the crystal phase at 59.7°C, which signifies monotropic behaviour for this compound. Similar phase transitions with a similar textural pattern and monotropicity are also observed for compounds **3h** and **3i**. Compound **3b** shows endothermic peaks at 65.0, 128.7 and 164.7°C, with enthalpies at 10.2, 19.6 and 14.0 kJ mol^{-1}. The exothermic peak observed at 112.2 defines the isotropic-to-crystal phase transition. The optical analysis displayed no texture either in the heating or the cooling cycles.

Thus, compound **3c** with $m = 8$ shows only the monotropic nematic pattern, whereas the higher members with $m > 8$ show a SmA mesophase due to the stronger additional intramolecular forces between the phenolic OH group and the nitrogen atom in the unsymmetrical azines. The additional intramolecular forces dominate in the higher homologues with anisotropic forces stabilising the mesophase.

The metal complexes of N-(*o*-hydroxybenzylidene)-N′-(4-n-alkoxy benzylidene)azines were found to be non-mesogenic, with almost the same clearing temperature independent of the carbon chain length. Thus, in the metal complexes chain length apparently plays no role in the isotropic temperature or the polymorphism. The non-mesogenic property of the metal complexes may be due to the symmetrical and rigid geometry of the metal complexes along with the stronger interaction of the potential donor (C=N) with a metal ion in the neighbouring layers. This results in the packing of molecules in the solid state, whereas the mesogenic nature of the azines persisted due to unsymmetrical and non-rigid geometry, leading to the involvement of intermolecular forces producing nematic and SmA patterns.

6. Conclusions

A new series of mesogenic unsymmetrical azines from salicylhydrazone derivatives, having terminal alkoxy chains ($m = 6 \sim 16$) and copper (II) complexes, has been synthesised. The chemical structure of the final products were investigated by FT-IR, far IR, UV–visible spectroscopy, ^{1}H and ^{13}C NMR spectra, ESR and magnetic susceptibility measurements. The mesomorphic properties and optical textures of the product were characterised by DSC and polarising

optical microscopy. The existence of the nematic and SmA phases was confirmed by the observation of schlieren and focal-conic textures in the optical microscopic cooling cycle. It was found that the unsymmetrical azines, N-(*o*-hydroxybenzylidene)-N′-(4-n-alkoxybenzylidene)azines, show mesomorphic properties, whereas their copper (II) complexes were non-mesogenic in nature and showed isotropic phases at higher temperatures ~180°C.

Acknowledgements

The authors thank the Head of the Department of Chemistry, Banaras Hindu University (BHU), Varanasi, for providing laboratory facilities. One of the authors (AP) thanks University Grants Commission, New Delhi (UGC) for financial support as a Project Fellow and the BHU for the research scholarship. Thanks are also due to Mr Satish Tiwari for CHN analyses, Mr R.C.P. Bipin for NMR and Mr V.N. Pandey for IR and electronic spectral data. We are thankful to S.A.I.F., Indian Institute of Technology (IIT), Bombay, for recording the ESR spectra.

Downloaded At: 14:08 25 January 2011

References

[1] Dragancea, D.; Arion, V.B.; Shova, S.; Rentschler, E.; Gerbeleu, N.V. *Angew. Chem. Int. Ed. Engl.* **2005**, *44*, 7938–7942.
[2] Rajeswaran, M.; Blanton, T.N.; Giesen, D.J.; David, R.W.; Nicholas, Z.; Brian, J.A.; Marcus, M.N.; Scott, T.M. *J. Solid State Chem.* **2006**, *179*, 1053–1059.
[3] Schweizer, E.E.; Cao, Z.; Rheingold, A.L.; Bruch, M. *J. Org. Chem*. **1993**, *58*, 4339–4345.
[4] Marek, R.; Stástná-Sedlácková, I.; Jousek, J.; Marek, J.; Potacek, M. *Bull. Soc. Chim. Belg.* **1997**, *106*, 645–649.
[5] Demus, D.; Goodby, J.; Gray, G.W.; Spiess, H.W.; Vill, V., *Handbook of Liquid Crystals*; Wiley VCH, Weinheim, 1998.
[6] Khodair, A.I.; Bertrand, P. *Tetrahedron* **1998**, *54*, 4859–4872.
[7] Yiang, Z.; Zheng, J.; Yang, C. *J. Lanz. Univ., J. Sichuan Union Univ., Eng. Sci. Ed.* **2004**, *40*, 51–54.
[8] Hoelzemann, G. *Expert Opin. Ther. Pat.* **2006**, *16*, 1175–1178.
[9] Screda, S.V.; Antipin, M.Y.; Timofeeva, T.V.; Struchkov, Y.T.; Sov, Y.T. *Phys. Crystallogr.* **1988**, *33*, 66–70.
[10] Astheimer, H.; Watz, L.; Haase, W.; Loub, J.; Muller, H.J.; Gallardo, M. *Mol. Cryst. Liq. Cryst*. **1985**, *131*, 343–351.
[11] Centore, R.; Panunzi, B.; Tuzi, A.Z. *Kristallog.* **1996**, *211*, 31–38.
[12] Centore, R.; Garzillo, C. *J. Chem. Soc. Perkin 2* **1997**, 79–84.
[13] Espinet, P.; Etxebarria, J.; Remon, A.; Serrano, J.L. *Angew Chem. Int. Ed. Engl.* **1989**, *28*, 1065–1066.
[14] Melendez, E.; Serrano, J.L. *Mol. Cryst. Liq. Cryst*. **1983**, *91*, 173–185.
[15] Marcos, M.; Melendez, E.; Ros, B.; Serrano, J.L. *Can. J. Chem*. **1985**, *63*, 2922–2925.
[16] Marcos, M.; Melendez, E.; Serrano, J.L. *Mol. Cryst. Liq. Cryst.* **1983**, *91*, 157–172.
[17] Centore, R.; Panunzi, B.; Roviello, A.; Sirigu, A.; Villano, P. *Mol. Cryst. Liq. Cryst.* **1996**, *275*, 107–120.
[18] Kesslen, E.C.; Euler, W.B. *Tetrahedron Lett.* **1995**, *36*, 4725–4728.
[19] Euler, W.B. *Handbook of Organic Conductive Molecules and Polymers, Vol. 2, Conductive Polymers: Synthesis and Electrical Properties*; Wiley, New York, 1997; pp 719–740.
[20] Chen, G.S.; Anthamatten, M.; Barnes, C.L.; Glaser, R. *Angew. Chem. Int. Ed. Engl*. **1994**, *33*, 1081–1083.
[21] Chen, G.S.; Wilbur, J.K.; Barnes, C.L.; Glaser, R. *J. Chem. Soc. Perkin Trans.* 2 **1995**, 2311–2317.
[22] Glaser, R.; Chen, G.S.; Anthamatten, M.; Barnes, C.L. *J. Chem. Soc. Perkin Trans. 2* **1995**, 1449–1458.
[23] Deun, R.V.; Parac-Vogt, T.N.; Hecke, K.V.; Meervelt, L.V.; Binnemans, K.; Guillon, D.; Donnio, B. *J. Mater. Chem.* **2003**, *13*, 1639–1645.
[24] Wilfrid, G.S.; Glenn, H.B. *J. Am. Chem. Soc*. **1959**, *81*, 2532–2537.
[25] Chudgar, N.K.; Sharma, H.C.; Shat, A.M. *Mol. Cryst. Liq. Cryst. Sci. Technol. C* **1996**, *6*, 1–6.
[26] Wei, Q.; Shi, L.; Cao, H.; Wang, L.; Yang, H.; Wang, Y. *Liq. Cryst.* **2008**, *35*, 581–585.
[27] Vill, V. *Liquid Crystals. 4.4-Database of Liquid Crystalline System Engineering (FQs)*; Fukuoka: Japan, 2003.
[28] Takahashi, H.; Kubo, K.; Takechi, H.; Matsumoto, T.; Ideta, K. *J. Oleo. Sci.* **2006**, *55*, 483–486.
[29] Khandar, A.A.; Rezvani, Z. *Polyhedron*, **1998**, *18*, 129–133.
[30] Rezvani, Z.; Ahar, R.; Nejati, K.; Seyedahmadian, S.M. *Acta Chim. Slov.* **2004**, *51*, 675–686.
[31] Rezvani, Z.; Abbasi, A.R.; Najati, K.; Seyedahmadian, S.M. *Polyhedron* **2005**, *24*, 1461–1470.
[32] Rezvani, Z.; Divband, B.; Abbasi, A.R.; Nejati, K. *Polyhedron* **2006**, *25*, 1915–1920.
[33] Lee, M.; Yoo, Y.S.; Chol, M.G. *Macromolecules* **1999**, *32*, 2777–2782.
[34] Shaw, D. *Fourier Transform N.M.R. Spectroscopy – Varian Associates Ltd., Walton-on-Thames*; Elsevier Scientific Publishing Company, New York, 1976; Chapter 8, pp. 203–268.
[35] Eaton, D.R.; Philips, W.D. *Adv. Magn. Res*., **1965**, *4*, 103.
[36] Temel, H.; Ilhan, S.; Sekerci, M.; Ziyadanogullari, R. *Spectr. Lett.* **2002**, *35*, 219–228.
[37] Larin, G.M.; Zvereva, G.A. *Russ. Chem. Bull. Int. Ed*., **2001**, *50*, 413–417.
[38] Guillon, E.; Oliver, D.; Barbier, J.P. *Polyhedron* **1998**, *17*, 3255–3261.
[39] Sawada, T; Fukumaru, K.; Sakurai, H. *Chem. Pharm. Bull*. **1996**, *44*, 1009–1016.
[40] Bertini, I; Dei, A; Scozzafava, A. *Inorg. Chem.* **1975**, *14*, 1526–1528.